Nanomed. J., 4(2): 107-114, Spring 2017

ORIGINAL RESEARCH PAPER

Evaluation of morphology and cell behaviour of a novel synthesized electrospun poly(vinyl pyrrolidone)/poly(vinyl alcohol)/hydroxyapatite nanofibers

*Raheleh Faridi-Majidi, Nader Nezafati *, Mohammad Pazouki, Saeed Hesaraki*

Nanotechnology and Advanced Materials Department, Materials and Energy Research Center, Karaj, Alborz, Iran

ABSTRACT

Objective(s): Three-dimensional structures such as nanofibrous scaffolds are being used in biomedical engineering as well as provide a site for cells to attach and proliferate leading to tissue formation. In the present study, poly(vinyl pyrrolidone) (PVP)/ poly(vinyl alcohol)(PVA) hybrid nanofibrous scaffold was synthesized by electrospinning.

Materials and Methods: The effect of adding nano hydroxyapatite (n-HA) and also Epoxypropoxy-propyl-trimethoxysilane (EPPTMS) as a crosslinking agent on morphology and cell behaviour of the nanofibers was investigated.

Results: Scanning electron microscope (SEM) observations showed that all kinds of nanofibers represented uniform and well-ordered morphologies without formation of any beads by controlling the synthesis parameters. The average ûber diameter of PVP-PVA was 260 nm. n-HA was synthesized by wet chemical process. The synthesized n-HA was characterized by XRD for structural analysis. Transmission electron microscope (TEM) revealed that HA particles had nanosized dimensions (in the range of 40-100 nm). The presence of n-HA within electrospun PVP-PVA nanofibers was confirmed by XRD and Fourier transmission infrared spectroscopy (FTIR) analyses. The average ûber diameter was decreased to 136 nm when n-HA was added in the composition of PVP-PVA. FTIR analysis depicted that PVP-PVA nanofibers were linked to EPPTMS as a biocompatible material by the covalent bond. Although adding n-HA caused to decrease the diameter of PVP-PVA nanofibers, addition of EPPTMS within PVP/PVA/n-HA nanofibers induced increasing distribution of fiber diameter as it enhanced to 195nm. In addition, the proper proliferation of G292 osteoblastic cells without any cytotoxicity was observed for the nanofiber.

Conclusion: Since these materials have been known as biomaterials, PVP/PVA/n-HA-EPPTMS nanofibers can be propounded as a good candidate for bone tissue engineering application.

Keywords: *Cytotoxicity, Electrospinning, G292 cell proliferation, Nano hydroxyapatite, Poly(vinyl pyrrolidone), Poly(vinyl alcohol), Silane agent*

How to cite this article

Faridi-Majidi R, Nezafati N, Pazouki M, Hesaraki S. Evaluation of morphology and cell behaviour of a novel synthesized electrospun poly(vinyl pyrrolidone)/poly(vinyl alcohol)/hydroxyapatite nanofibers. Nanomed J. 2017; 4(2): 107-114.
DOI: 10.22038/nmj.2017.22112.1236

INTRODUCTION

Tissue engineering represents an interdisciplinary field with the aim of tissue regeneration [1]. Tissue engineering technique is the ability to restore or improve tissue function [2]. Scaffolds such as gels, nano/micro fibers, films, and membranes have been evaluated as dermal and bone substitutes [3, 4]. Among the available scaffolds, nanofibers are promising candidates since they mimic the native extracellular matrix (ECM), own have high porosity, large surface area-to-volume ratio, which allows cell proliferation and could be surface modified. Polymeric nanofibers are gaining popularity in tissue engineering and have been used in attempts to regenerate a variety of tissues [5].

Electrospinning is a method of generating fibers with diameters on the order of nanometers to

*Corresponding Author Email: *n.nezafati@merc.ac.ir*
Tel: (+98) *03536235715*

Note. This manuscript was submitted on January 18, 2017; approved on February 28, 2017

micrometers. The geometric properties of electrospun fibers are easily tuned as well [6].

Poly(vinyl alcohol) (PVA) is a well-known biological friendly polymer due to its important features such as high hydrophilicity, non-toxicity, recognized biodegradability and biocompatibility [7, 8]. PVA blends can be utilized as functional materials including biomedical materials such as dialysis membranes, wound dressing, artificial skin, cardiovascular devices and as vehicles to release active substances in a controlled manner [7].

Polyvinyl pyrrolidone (PVP) has a good eminence because of its interesting absorption and complexes abilities [9]. The use of PVP in medicine and topical applications onto the skin for the transdermal delivery of drugs has been described as well [10, 11]. Moreover, PVP is a vinyl and an amorphous polymer possessing planar and highly polar side groups due to the peptide bond in the lactam ring [12]. Therefore, it is known to form various complexes with other polymers.

Polymer blending is a useful technique and one of the most important ways for the development and designing new polymeric materials with a wide variety of properties [13]. The notable advantages of polymer blends are that the properties of the final product can be handled to the requirements of the applications, which cannot be acquired alone by one polymer [13].

PVA and PVP as synthetic polymers are water soluble. A hydrogen-bonding interaction between these two polymers [12] and intramolecular hydrogen bonds within PVA are responsible for the solubility of PVA and PVP in water [12]. Nevertheless, this characteristic could be a disadvantage because the material would dissolve in contact with fluids into the human body [8]. For that reason, the appropriate chemical cross-linking improves their stability in the aqueous media to consider as long term implants. Dialdehydes, dicarboxylic acids, dianhydrides are some examples that have been recently utilized for PVA and PVP modification [14-16].

Hydroxyapatite (HA) [$Ca_{10}(PO_4)_6(OH)_2$] is known to be biocompatible, bioactive (i.e. having an ability to form a direct chemical bond with surrounding tissues), osteoconductive, non-toxic, non-infiammatory and non-immunogenic [17]. It is also the major inorganic material that constitutes the hierarchical structure of bone and teeth [18].

According to the abovementioned explanations, this study is to evaluate the effect of adding epoxypropoxy-propyl-trimethoxysilane (EPPTMS) as a biocompatible crosslinker and also nano hydroxyapatite (n-HA) on morphology, chemical groups and phase analysis of the electrospun PVA-PVP nanofibers. These nanofibers, as candidates for bone tissue engineering, were characterized using proper analytical techniques such as scanning electron microscope (SEM) and Fourier transform infrared spectroscopy (FTIR) and X-ray diffraction (XRD).

MATERIALS AND METHODS

Materials

Polyvinylpyrrolidone [PVP; $(C_6H_9NO)_n$, Rahavard Tamin Co. (Iran), CAS No. 9003-39-8; $M_W=1.3\times10^5$], poly(vinyl alcohol)[PVA; $[CH_2CH(OH)]_n$, JP-20Y (Japan), MSDS No.07-03E; Avg. Mw=30000-70000] and EPPTMS [Merck, 8418070100] used as main raw materials for the synthesis of nanofibrous mats.

Preparation of PVA-PVP solution with/without n-HA

The equal amounts of PVA and PVP were dissolved in distilled water to obtain a polymeric solution with concentration of 10% (w/v). n-HA powder was synthesized according to our previous work [13]. Afterwards, HA powder was added to the solution as the weight ratio of HA to PVA-PVP was 0.1. The solution was ultrasonically stirred for 3 h at 25æ%C to obtain a homogeneous solution.

Preparation of EPPTMS crosslinked PVA-PVP/n-HA solution

The polymeric solution containing n-HA was prepared similar to section 2.2. 20 wt% (with respect to the weight of PVA-PVP) of EPPTMS was then added to the solution. After that, the solution was ultrasonically stirred for 5 h at 25æ%C to obtain a homogeneous solution. The ratio of HA to PVA was selected similar to section 2.2.

Electrospinning of the solution

The resultant three types of solutions were poured into standard 5mL syringes containing 18-gauge blunt-tip needles. The size of aluminum foil was also considered 10×10 cm. The most appropriate conditions for electrospinning of the solutions were selected when the nozzle-collector distance was

160mm, voltages and flow rates were varied from 18 to 22 kV and 1mmh^{-1}, respectively. After electrospinning process (by electrospinning device of Fanavaran Nanomeghyas Co. (Model ES1000), Iran) was completed, the obtained mats were dried at room temperature for 24h.

Characterization of the electrospun nanofibers

Morphological characterization of the nanofibers and n-HA was performed using SEM [Vega II Tescan, Czech] and FE-SEM [Mira3-Tescan, Czech], respectively, operated at an acceleration voltage of 10 kV. Before testing, the samples were coated with a thin layer of gold (Au) by a sputtering apparatus. The chemical groups of the samples were examined by a Perkin Elmer 400 spectrometer. For FTIR analysis, initially, 1 mg of the scraped sample was carefully mixed with 300 mg of KBr (infrared grade) and palletized under vacuum. Then the pellets were analyzed in the range of 4000-400 cm^{-1} with a scan rate of 23scan/min and a resolution of 4 cm^{-1}. The diameter and diameter distribution of the nanofibers were determined by using Image J software (1.44p/Java 1.6.0_20 (32-bit)) with sampling sizes of at least 40 fibers from the SEM micrograph. To see the major phase of the nanofibers and n-HA, phase analysis was performed by a Philips PW3710 diffractometer with voltage and current settings of 40 kV and 30 mA, respectively. Cu-K$_{á}$ radiation was also used for the microsphere (1.54 Å). X-ray diffraction (XRD) diagrams were also recorded in the interval 10^{o} d" 2é d" 80^{o} at the scan speed of 2^{o}/s.

Cellular responses to the electrospun nanofibers

To evaluate the biological properties of PVA-PVP/n-HA nanofibers, two hundred microliters of G292 osteoblastic cells suspension (3×10^{4} cells/mL) was slowly dispersed over the top surface of nanofiber-coated cover slips placed in a 24-well culture plate and cultivated in a minimum modified eagle medium (MEM) (Biochrom, Berlin, Germany) containing 10% fetal calf serum (Biochrom), 100U/ml penicillin (Merck), streptomycin (70 mg/mL), gentamycin (120 mg/mL), and amphotericin B (3 mg/mL) in a 5%CO_2 atmosphere at 37ÚC. Cells cultured in a blank well were used as a control. Seeded cells were cultured for 48h and the medium was changed every day. MTT (3-(4, 5-dimethylthiazol-2-yl)-2, 5-diphenyl-tetrazolium bromide) assay was performed to determine the number of viable cell in the nanofibers. MTT was taken up by active cells and reduced in the mitochondria to insoluble purple formazan granules. Subsequently, the medium was discarded and the precipitated formazan was dissolved in dimethyl sulfoxide, DMSO, (150 ml/well), and optical density of the solution was read using a microplate reader (ELx808, Biotek ®) at a wavelength of 570 nm [19].

Moreover, in order to assess *in vitro* cytotoxicity of the nanofiber, the cells were observed after 48h under optical microscopy (Olympus CKX41). Cellular responses were scored as 0, 1, 2 and 3 according to non-cytotoxic, mildly cytotoxic and severely cytotoxic as per ISO 10993-5.

RESULTS AND DISCUSSION

Fig. 1 depicts the microstructure of electrospun PVA/PVA, PVA/PVP/n-HA and PVA/PVP/n-HA-EPPTMS with two different magnifications (Figs 1(a) to 1(f), respectively). As it can be seen, all samples represent uniform fibers without the formation of any beads. In fact, adding n-HA and EPPTMS in the structure of electrospun PVA/PVA does not influence a bad effect in term of uniformity of the fibers. Increasing the

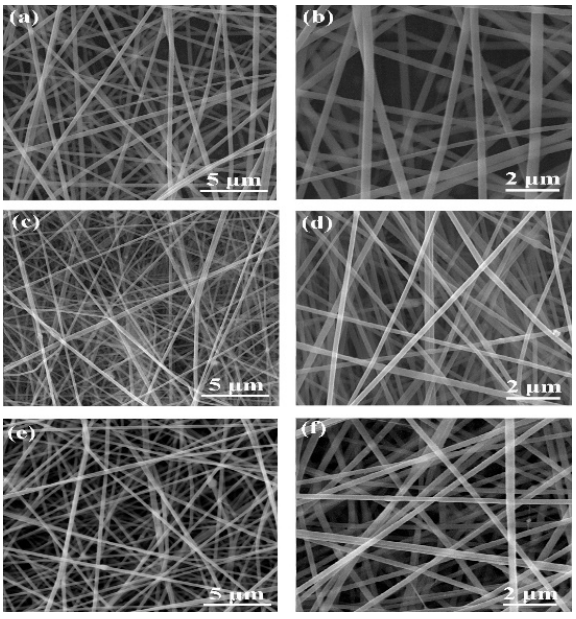

Fig. 1. The microstructure of electrospun: PVA/PVA (a), PVA/PVA (high magnification 10 kX) (b), PVA/PVP/n-HA (c), PVA/PVP/n-HA (high magnification 10 kX) (d), PVA/PVP/n-HA-EPPTMS (e) and PVA/PVP/n-HA-EPPTMS (high magnification 10 kX) (f)

concentration of the polymeric solution (up to a critical value) will lead to an increase in the viscosity, which then increases the chain entanglement among the polymer chains. These chain entanglements overcome the surface tension and ultimately result in uniform beadless electrospun nanofibers [20]. In other words, complex of PVA-PVP and n-HA in spinning along with EPPTMS formed a similar structure with a branched polymer, which increased the resistance against the drawing tension when PVA-PVP chains were oriented by the tension loaded during the spinning process. This tension-stiffening phenomenon had the advantage of diminishing a local stress concentration effect arising from an unstable drawing fow. Thus, it is possible to prepare uniform fbers without breakage of the fibers during the spinning process [21]. There are many factors such as solution viscosity and surface tension impact on bead formation. Bead formation can be due to the solution viscosity that can be governed by controlling solution concentration. High surface tension can lead to form small droplets along the fibers as well. It can cause bead formation instead of fibers reducing uniformity of electrospun fibers [21]. In overall, two main reasons can reduce bead formation in fibers: First, reducing attractive and repulsive forces on Taylor's cone that increases uniformity of fibers and second, increasing flight time that leads to increasing evaporation of solvent [22].

The fiber size distribution of the nanofibers has been shown in Fig .2. As it can be seen the electrospun PVA/PVA nanofibers possess diameters in the range of 110–370 nm and the average fiber diameter is on the order of 260 nm (Fig 2(a)). On the other hand, the diameter of nanofibers (with the range of 60 to 330 nm) and also average fiber diameter (136 nm) was decreased when n-HA was added in the composition of PVA-PVP (Fig 2 (b)). In fact, adding ionic materials such as n-HA within the polymeric solution of PVA-PVP tunes and increases the electrical conductivity of the solution. This is in accordance with the other work as well [23]. Therefore, according to the other researches, with the aid of ionic salts and/or hydroxyapatite in polymeric solutions, nanofibers with small diameter can be obtained [24, 25].

It is worth to note that by adding EPPTMS as a crosslink agent, the fiber diameter is increased with respect to fiber diameter of PVA/PVP/n-HA (Fig 2(c)). The average fiber diameter is on the order of 195 nm. This can be due to strong effect of EPPTMS on the PVA-PVP chain entanglement and inter- or intra-molecular interactions.

The reason is in good agreement with other research concerning electrospun poly(acrylic acid) nanofibers crosslinked with cellulose nanocrystal [26].

Fig. 3 displays the FE-SEM micrograph (Fig 3(a)) along with X-ray pattern (Fig 3(b)) of hydroxyxapatite nanoparticles (n-HA). The micrograph represents the formation of spherical to flake-like particles with some degrees of agglomeration. It can be also seen that the grain size range for n-HA is 40-100 nm. The

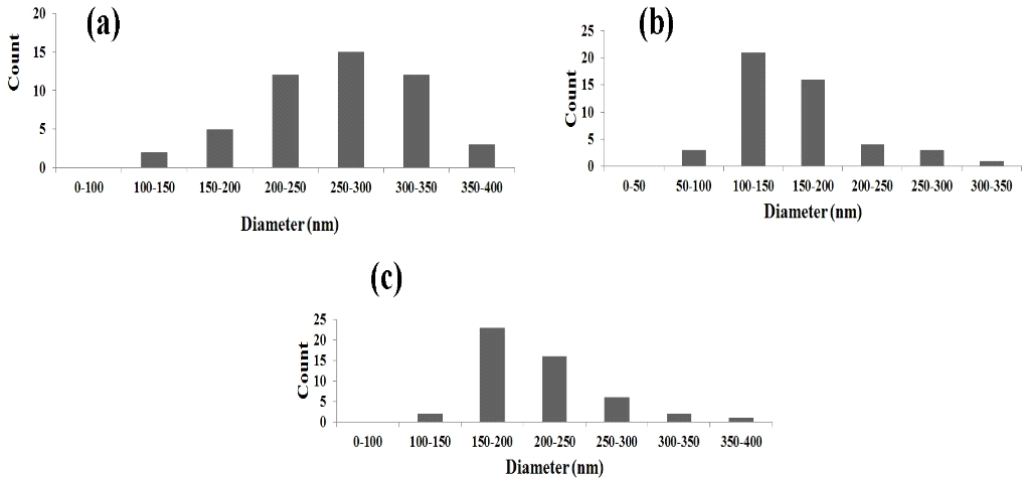

Fig. 2. The fiber size distribution of: PVA/PVA (a), PVA/PVP/n-HA (b) and PVA/PVP/n-HA-EPPTMS (c) nanofibers

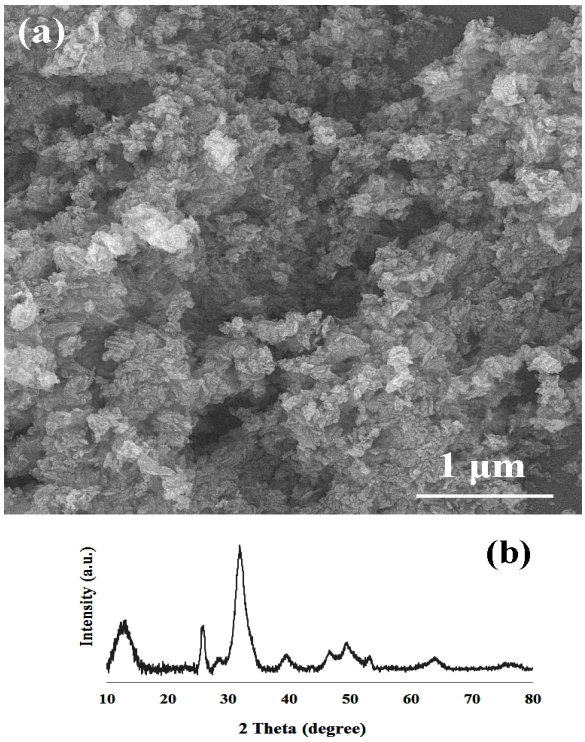

Fig. 3. The FE-SEM micrograph (a) along with X-ray pattern (b) of hydroxyxapatite nanoparticles (n-HA)

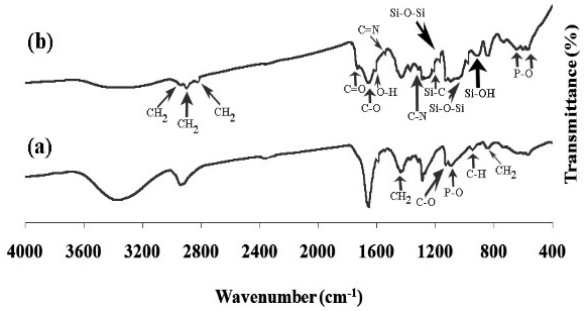

Fig. 4. FTIR of: PVA/PVP/n-HA (a) and PVA/PVP/n-HA-EPPTMS (b) electrospun nanofibers

XRD pattern of the n-HA reveals that the characteristic peaks of n-HA have been located at 25.85°, 28.7°, 32°, 39.4°, 46.8°, 49.4°, 51° and 61° relates to the (200), (002), (210), (211), (300), (202), (222), (213), (004), (320) and (304) reflection planes of HA phase, respectively. It can be concluded that these peaks of HA diffraction patterns agree with those of standard HA in the powder diffraction file (JCPDS No. 09-432) which shows the typical hydroxyapatite patterns and second phase was not detected.

The results of FTIR of PVA/PVP/n-HA and PVA/PVP/n-HA-EPPTMS have been shown in Fig. 4. In both samples (Figs. 4(a) and (b)), the spectrum corresponding to HA appearing at 1655 cm^{-1} represent the hydroxyl vibrations, whereas peaks located at 1050 cm^{-1}, 640 cm^{-1} and 570 cm^{-1} belong to the bending and stretching of phosphate group [27]. However, as it can be seen from the Figs, the OH vibration peak at 1377 cm^{-1} which is related to pure HA has been disappeared.

This may be due to intermolecular interaction between HA and PVA/PVP matrix, especially in the form of hydrogen bond interaction, just as Gonzalez indicated in literature [28].

The absorption band at 970 cm^{-1} is assigned to the out-of-plane rings C-H bending [29, 30]. A characteristic alcohol band at 1095 cm^{-1} is assigned to the stretching of C-O of PVA which is influenced by hydrogen bonding along with C-H and O-H bending. Characteristic C-N stretching vibrations of PVP were observed at 1280 and 1305 cm^{-1} [31, 32]. The band at about 1285 cm^{-1} corresponds to C-O stretching of acetyl groups present on the PVA backbone. The absorption peaks at 1430 cm^{-1} (CH_2 bending) and 840 cm^{-1} (CH_2 rocking) characteristic to PVA manifest in all spectra. A small absorption band at about 1539 cm^{-1} is related to the characteristic vibration of C=N (pyridine ring) [32].

The vibration band at about 1655 cm^{-1} corresponds to C-O symmetric bending [34] of PVA and PVP. Another band at 1730 cm^{-1} is attributed to the stretching vibration of C = O of PVP. The band corresponding to CH_2 asymmetric stretching vibration of PVA+PVP blend appeared around 2930 cm^{-1}. FTIR image (Fig. 4(b)) of PVA/PVP/n-HA-EPPTMS reveals that similar to the sample PVA/PVP/n-HA, the peaks of PVA, PVP and HA groups are also observed. Furthermore, there is also bands at about 1030 (cm^{-1}) and 1150 (cm^{-1}) that represented Si-O-Si crosslinking bands. There is a stretching band of Si-OH at about 920 (cm^{-1}) as well [35].

A successful crosslinking PVA/PVP/n-HA with EPPTMS is affirmed due to the presence of Si-O-Si and Si-OH bands. In fact, the end of silane group in EPPTMS participated in formation of silica network [36]. Moreover, the presence of resonance at about 1265 (cm^{-1}) related to Si-C stretching band [37] along with the weak resonances at the ranges of 2840 (cm^{-1})

and 2920 (cm^{-1}) related to CH_2 stretching vibration band (emanates from methyl groups of EPPTMS) are another reason for proper crosslinking PVA/PVP/n-HA with EPPTMS.

Fig. 5 shows the XRD pattern of the PVA blend with PVP containing n-HA and EPPTMS. The characteristic peaks of both PVA and PVP agreed with the reported results [37]. It is certain that PVA is a semi-crystalline polymer with regions of structural order and disorder showing a diffraction peak 2θ around 19.8°. However, PVP is an amorphous polymer forming a miscible blend with PVA. The peak of PVP reveals a couple of broad bands located at 2θ = 11° and 22° [31, 38]. Blending of these two polymers is important to maintain the desired mechanical and hydrophilic character of the nanofibers. Moreover, the diffraction characteristic peaks that appear at around 26°, 32° and 40° correspond to the peaks of the n-HA powder [39]. It seems that n-HA filled in the gap of PVA-PVP network which emanates from motion of polymer blend chains in the amorphous region [40]. The XRD result also represents that the presence of silane-coupling agent EPPTMS does not indicate any measurable diffraction peaks and therefore, by adding EPPTMS in the structure, no detectable change is observed.

The cytotoxicity study of control sample and PVA/PVP/n-HA-EPPTMS nanofiber was assessed. The assay results showed that the nanofiber had no cytotoxic leachables when compared to control (Figs. 6 a and 6 b). The test also depicted that the cells appeared spindle in shape and formed a monolayer. The cytotoxic scale was measured as zero, which corresponds to non-cytotoxicity of sample. MTT assay showed nearly 80% viability of G292 cells and reasonable proliferation of cells (Fig. 7) after 48 h of culture on a PVA/PVP-nHA nanofibers film (n=3) wrapped cover slips when compared to the control.

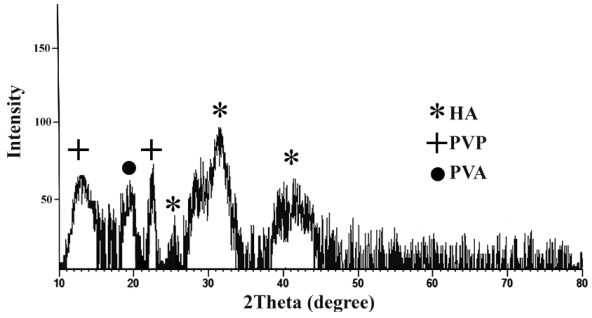

Fig. 5. The XRD pattern of the PVA/PVP/n-HA-EPPTMS electrospun nanofibers

In overall, according to the results, the electrospun PVA/PVP/n-HA-EPPTMS nanofiber can be propounded as a potential bone filler similar to the other calcium phosphate-based materials (i.e.: beta tricalcium phosphate [β-TCP] bone graft, calcium phosphate cements [CPCs] and etc.) because they provide a good environment to penetrate the cells into the bone defects. However, it is worth to note that the abovementioned materials have a weak mechanical properties and can be only used in non-

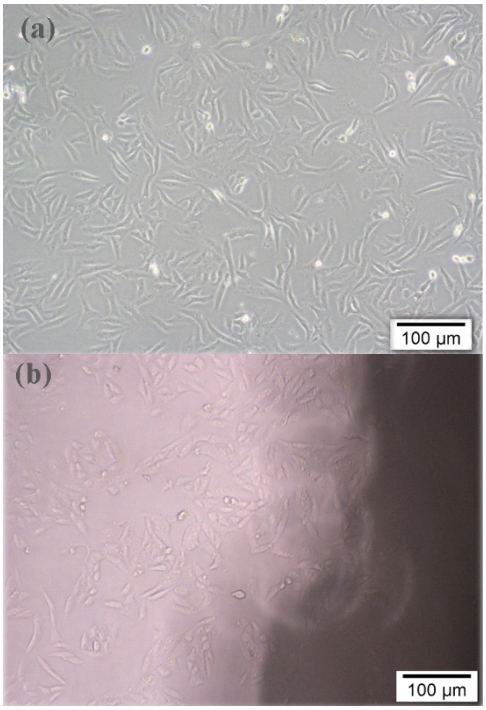

Fig. 6. Optical micrograph of: control (a) and PVA/PVP/n-HA-EPPTMS nanofibers (b) after 2 days of G292 cell culture

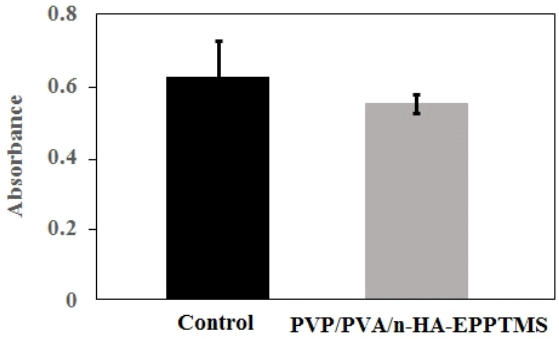

Fig. 7. The proliferation of G292 cell cultured on PVA/PVP/n-HA-EPPTMS nanofibrous scaffold for two days

load bearing sites. Therefore, the mechanical support can be provided by surrounding bone hard tissue or other fixation devices such as plates and screws.

CONCLUSIONS

In this study, the morphological evaluation of 50PVA-50PVP electrospun nanofibers was assessed and compared to that of samples with n-HA and EPPTMS as a crosslinking agent as well.

Morphological observations described that all nanofibers had appropriate smoothness and uniformity whereas no beads were formed. It was also revealed that the fiber diameter of 50PVA-50PVP blends decreased by adding n-HA. On the other hand, by adding EPPTMS, the diameter and diameter distribution of the nanofibers were increased with respect to polymer solution of PVA-PVP containing n-HA. Addition of EPPTMS and n-HA did not influence the adverse effect on morphology of the nanofibers. The presence of CH_2 asymmetric stretching vibration related to PVA+PVP blending, the intermolecular interaction between HA and PVA/PVP matrix and also a proper crosslinking PVA/PVP/n-HA with EPPTMS were confirmed by FTIR.

X-ray pattern demonstrated the diffraction characteristic peaks of n-HA and both PVA and PVP whereas no detectable change was observed after adding EPPTMS in the structure. Based on and MTT assay, the result suggested that the nanofiber was non-toxic and the G292 cells could proliferate appropriately in the presence of the nanofiber as well. In conclusion, the PVA/PVP/n-HA-EPPTMS nanofiber might be considered as potential candidate for use in tissue engineering as a bone filler.

ACKNOWLEDGMENTS

This outcome has been achieved by electrospinning device of Fanavaran Nano-Meghyas Co. (model ES100). Special thanks belong to the Fanavaran Nano-Meghyas Company where the nanofibers were prepared.

The authors would also like to thank cell culture laboratory of Materials and Energy Research Center (MERC) for its help to perform cell culture procedure.

CONFIICT OF INTEREST

The authors declare that there are no conflicts of interest.

REFERENCES

1.Yang F, Murugan R, Wang S, Ramakrishna S. Electrospinning of nano/micro scale poly (L-lactic acid) aligned fibers and their potential in neural tissue engineering . Biomaterials. 2005; 26(15): 2603-2610.

*2.*Liao S, Murugan R, Chan C, Ramakrishna S. Processing nanoengineered scaffolds through electrospinning and mineralization suitable for biomimetic bone tissue engineering. J Mech Biomed Mater. 2008; 1(3): 252-260.

3. Sundaramurthi D, Krishnan UM, Sethuraman S. Electrospun nanofibers as scaffolds for skin tissue engineering. Polym Rev. 2014; 54 (2): 348–376.

4. Yi H, Rehman FU, Zhao C, Liu B, He N. Recent advances in nano scaffolds for bone repair. Bone Res. 2016; 4, 16050, 1-11.

5. Barnes CP, Sell SA, Boland ED, Simpson DG, Bowlin GL. Nanofiber technology: designing the next generation of tissue engineering scaffolds. Adv Drug Deliv Rev. 2007; 59(14): 1413-1433.

6. Schaub NJ, Le Beux C, Miao J, Linhardt RJ, Alauzun JG, Laurencin D, Gilbert RJ. The Effect of Surface Modification of Aligned Poly-L-Lactic Acid Electrospun Fibers on Fiber Degradation and Neurite Extension. Plos One. 2015; 10(9): 0136780, 1-19.

7. Seabra AB, de Oliveira MG. Poly (vinyl alcohol) and poly (vinyl pyrrolidone) blended films for local nitric oxide release. Biomaterials. 2004; 25(17): 3773–3782.

8. Nakhaei O, Shahtahmassebi N. Study structural and up-conversion luminescence properties of polyvinyl alcohol/ CaF_2:erbium nanofibers for potential medical applications. Nanomed J. 2015; 2(2): 160-166.

9. Sionkowska A, Wisniewski M, Kaczmarek H, Skopinska J, Chevallier P, Mantovani D, Lazare S, Tokarev V. The influence of UV irradiation on surface composition of collagen/PVP blended films. Appl Surf Sci. 2006; 253(4): 1970-1977.

10. Lopes CMA, Felisberti MI. Mechanical behavior and biocompatibility of poly(1-vinyl-2-pyrrolidone)-gelatin IPN hydrogels Biomaterials. 2003; 24(7): 1279–1284.

11. Wang Q, Hikima T, Tojo K, Skin penetration enhancement by synergistic of supersaturated dissolution and chemical enhancers. J Chem Eng Jpn. 2003; 36(1): 92–97.

12. Shanthi B, Muruganand S. Structural, vibrational, thermal, and electrical properties of PVA/PVP biodegradable polymer. Inter J Sci Eng Appl Sci. 2015; 1(8): 1105-1113.

13. Abdelrazek EM, Elashmawi IS, El-khodary A, Yassin A. Structural, optical, thermal and electrical studies on PVA/PVP blends filled with lithium bromide. Curr App Phys. 2010; 10(2): 607–613.

14. Sun M, He Y, Yang W, Yin M. A fluorescent perylene-assembled polyvinylpyrrolidone film: synthesis, morphology and nanostructure. Soft Matter. 2014; 10(19): 3426-3431.

15. Ahmad SI, Hasan N, Abid CKVZ, Mazumdar N. Preparation and Characterization of Films Based on Crosslinked Blends of Gum Acacia, Polyvinylalcohol, and Polyvinylpyrrolidone Iodine Complex. J Appl Polym Sci. 2008; 109 (2): 775–781.

16. Chatterjee PK, Gupta BS (Eds.). Absorbent Technology, Volume 13 of Textile Science and technology. Raleigh, N.C.: Elsevier; 2002, 500 pages.

17. Saber-Samandari S, Nezafati N, Saber-Samandari S. The Effective Role of Hydroxyapatite Based Composites in

Anticancer Drug Delivery Systems. Crit Rev Ther Drug. Carrier. Syst. 2016; 33(1): 41-75.

18. Haider A, Versace DL, Gupta KC, Kang IK. Pamidronic acid-grafted nHA/PLGA hybrid nanofiber scaffolds suppress osteoclastic cell viability and enhance osteoblastic cell activity. J Mater Chem B. 2016; 4(47): 7596-7604.
19. Nagiah N, Tiruchirapalli U, Mohan SR, Srinivasan NT, Sehgal PK. Development and Characterization of Electropsun Poly(propylene carbonate) Ultrathin Fibers as Tissue Engineering Scaffolds. Adv Eng Mater. 2012; 14 (4): 138-148.
20. Haider A, Haider S, Kang IK. Comprehensive review summarizing effect of electrospinning parameters and potential applications of nanofibers in biomedical and biotechnology. Arab J Chem. 2015; In Press, http://dx.doi.org/10.1016/j.arabjc. 2015.11.015.
21. Chung YS, Kang SI, Kwon OW., Shin DS, Lee SG, Shin EJ, Min BG, Bae HJ, Han SS, Jeon HY, Noh SK, Lyoo WS. J. Preparation of hydroxyapatite/poly(vinyl alcohol) composite fibers by wet spinning and their characterization. Appl Polym Sci. 2007; 106(5): 3423–3429.
22. Nezafati, N, Zamanian A. Effect of Silane-Coupling Agent Concentration on Morphology and In Vitro Bioactivity of Gelatin-Based Nanofibrous Scaffolds Fabricated by Electrospinning Method. J Biomater Tissue Eng. 2015; 5(1): 78-86.
23. Chaudhuri B, Mondal B, Ray SK, Sarkar SC. A novel biocompatible conducting polyvinyl alcohol (PVA)-polyvinylpyrrolidone (PVP)-hydroxyapatite (HAP) composite scaffolds for probable biological application. Colloids Surf. B Biointerfaces. 2016; 143, 71-80.
24. Huang C, Chen S, Lai C, Reneker DH, Qiu H, Ye Y, Hou H. Electrospun polymer nanofibres with small diameters. Nanotechnology. 2006; 17(6):1558–1563.
25. Fang R, Zhang E, Xu L, Wei S. J. Electrospun PCL/PLA/HA based nanofibers as scaffold for osteoblast-like cells. Nanosci. Nanotechnol. 2010; 10 (11): 7747-7751.
26. Lu P, Hsieh YL. Cellulose nanocrystal-filled poly(acrylic acid) nanocomposite fibrous membranes. Nanotechnology. 2009; 20(41): 1-9.
27. Chaudhuri B, Mondal B, Modak DK, Pramanik K, Chaudhuri BK. Preparation and characterization of nanocrystalline hydroxyapatite from egg shell and K_2HPO_4 solution. Mater Lett. 2013; 97,148–150.
28. Gonzalez JS, Alvarez VA. J. Mechanical properties of polyvinylalcohol/hydroxyapatite cryogel as potential artificial cartilage. Mech Behav Biomed. 2014; 34, 47-56.
29. Li X, Goh SH, Lai YH, Wee ATS. Miscibility of carboxyl-containing polysiloxane/poly(vinylpyridine) blends. Polymer. 2000; 41(17): 6563–6571.
30. Laot CM, Marand E, Oyama HT. Spectroscopic characterization of molecular interdiffusion at a poly(vinyl pyrrolidone)/vinyl ester interface. Polymer. 1999; 40(5): 1095–1108.
31. Rajendran S, Sivakumar M, Subadevi RJ. Effect of salt concentration in poly (vinyl alcohol)-based solid polymer electrolytes. J Power Sources; 2003; 124(1): 225-230.
32. Giri N, Natarajan RK, Gunasekaran S, Shreemathi S. 13C NMR and FTIR spectroscopic study of blend behavior of PVP and nano silver particles. Arch Appl Sci Res. 2011; 3(5): 624-630.
33. Abdelrazek EM, Elashmawi IS, Labeeb S. Chitosan filler effects on the experimental characterization, spectroscopic investigation and thermal studies of PVA/PVP blend films. Physica B Condens Matter. 2010; 405 (8): 2021–2027.
34. Wu HD, Wu ID, Chang FC. The interaction behavior of polymer electrolytes composed of poly(vinyl pyrrolidone) and lithium perchlorate ($LiClO_4$), Polymer. Polymer. 2001; 42(2), 555–562.
35. Davis SR, Brough AR, Atkinson A. Formation of silica/epoxy hybrid network polymers. J Non Cryst Solids. 2003; 315(1-2): 197-205.
36. Gizdavic-Nikolaidis M, Edmonds N, Bolt C, Easteal A. Structure and properties of GPTMS/DETA and GPTMS/EDA hybrid polymers. Curr Appl Phys. 2008; 8(3-4): 300-303.
37. Kokubo T, Kushitani H, Sakka S, Kitsugi T, Yamamuro T. Solutions able to reproduce in vivo surface-structure changes in bioactive glass-ceramic A-W. J Biomed Mater Res. 1990; 24(6): 721-734.
38. Zheng MP, Gu MY, Jin YP, Jin GL. Optical properties of silver-dispersed PVP thin film. Mater Res Bull. 2001; 36 (5-6): 853-859.
39. Huang X, Zuo Y, Li JD, Li Y.B. Study on crystallisation of nano-hydroxyapatite/polyvinyl alcohol composite hydrogel. Mater Res Innov. 2009; 13(2): 98-102.
40. Elashmawi IS, Baieth HEA. Spectroscopic studies of hydroxyapatite in PVP/PVA polymeric matrix as biomaterial. Curr Appl Phys. 2012; 12(1): 141-146.